

Swarm Intelligence Optimization of Multi-RIS Aided MmWave BeamSpace MIMO

Zaid Abdullah, Mario R. Camana, Abuzar B. M. Adam, Chandan K. Sheemar,
Eva Lagunas, and Symeon Chatzinotas

Interdisciplinary Centre for Security, Reliability and Trust (SnT), University of Luxembourg, Luxembourg.

Corresponding Author: Zaid Abdullah (Email: zaid.abdullah@uni.lu).

Abstract—We investigate the performance of a multiple reconfigurable intelligence surface (RIS)-aided millimeter wave (mmWave) beamSpace multiple-input multiple-output (MIMO) system with multiple users (UEs). We focus on a challenging scenario in which the direct links between the base station (BS) and all UEs are blocked, and communication is facilitated only via RISs. The maximum ratio transmission (MRT) is utilized for data precoding, while a low-complexity algorithm based on particle swarm optimization (PSO) is designed to jointly perform beam selection, power allocation, and RIS profile configuration. The proposed optimization approach demonstrates positive trade-offs between the complexity (in terms of running time) and the achievable sum rate. In addition, our results demonstrate that due to the sparsity of beamSpace channels, increasing the number of unit cells (UCs) at RISs can lead to higher achievable rates than activating a larger number of beams at the MIMO BS.

Index Terms—Multiple-input multiple-output (MIMO), BeamSpace MIMO, millimeter wave (mmWave), Reconfigurable intelligent surface (RIS), Particle swarm optimization (PSO).

I. INTRODUCTION

BeamSpace multiple-input multiple-output (MIMO) refers to systems in which data is multiplexed onto orthogonal spatial beams. One of the main advantages of beamSpace MIMO is the high sparsity manifested in the beamSpace channel matrix [1]. Thus, one can select only a small number of available beams without experiencing a large performance degradation in terms of the achievable sum rates [1], [2].

The fundamental difference between beam selection in beamSpace MIMO and antenna selection in conventional MIMO is as follows: In conventional MIMO systems, narrower beams are only possible if more antennas are selected. In contrast, the narrow beam widths in the beamSpace MIMO are preserved regardless of the number of selected beams (or radio-frequency (RF) chains). The reason is that in beamSpace MIMO, the base station (BS) is equipped with a discrete lens array (DLA) which behaves as a convex lens to direct signals toward different points of the focal surface. As such, it is feasible in beamSpace MIMO to achieve significant reductions in hardware complexity and power consumption without sacrificing the high antenna gains. Such properties make beamSpace MIMO particularly suitable for communications over higher frequency bands such as millimeter wave (mmWave) [2].

Another promising technology for high-frequency communications is the reconfigurable intelligent surface (RIS). An RIS is made up of a large number of tiny elements known as unit cells (UCs). Each UC manipulates the phase

of impinging signals, such that signals reflected by different UCs are added constructively at the receiving node. Therefore, one of the main advantages of RISs is that they can provide virtual communication links when the direct link between two communication nodes is blocked. In addition, the near-passive nature of RISs make them an attractive choice to maintain low levels of hardware complexity and power consumption [3].

To that end, we investigate the performance and optimization of multi-RIS-aided mmWave beamSpace MIMO systems. In particular, we design a low complexity optimization scheme to perform joint optimizations with respect to beam selection, power allocation, and RIS profile configuration. In addition, we adopt the low-complexity maximum ratio transmission (MRT) for data precoding. Works on RIS-aided beamSpace MIMO have been reported in [4]–[6]. Unlike our work, the authors in [4] considered a single user (UE) scenario, while the authors in [5] and [6] considered a single RIS scenario and modeled the channels between the RIS and UEs as Rayleigh fading, which is not realistic for practical mmWave systems.

Our main contributions can be summarized as follows: (i) We propose a beamSpace MIMO system with multiple UEs and distributed RISs. The presence of distributed RISs is crucial for providing additional paths leading to enhanced channels rank, and thereby enabling spatial multiplexing, (ii) We design a low-complexity particle swarm optimization (PSO) algorithm to jointly optimize the selected beams, allocated powers, and RIS phase profiles, and (iii) we study the trade-offs in terms of number of selected beams, number of UCs, number of UEs, as well as the complexity of the PSO algorithm on the sum rate performance.

The rest of this paper is organized as follows: System and channel models are described in Section II. In Section III we formulate the received signals, sum rate, and the optimization problem. The proposed PSO algorithm is explained in Section IV. Numerical results are presented in Section V. Finally, concluding remarks are in Section VI.

Notations: Matrices and vectors are represented by uppercase and lowercase boldface letters, respectively. The vectors \mathbf{x}_c and $\mathbf{x}_{z,c}$ denote the c th column of matrices \mathbf{X} and \mathbf{X}_z , respectively. The i th element of the vector \mathbf{x} is denoted by $[\mathbf{x}]_i$ with its absolute value denoted by $|[\mathbf{x}]_i|$, while $[\mathbf{X}]_{i,j}$ is the i th element of the j th column of \mathbf{X} . Assuming \mathbf{x} is an N -dimensional vector, $[\mathbf{x}]_{i:j}$ denotes the elements in \mathbf{x} indexed from i to j ($i < j < N$), while $[\mathbf{x}]_j$ refers to all

elements in \mathbf{x} indexed from j to N . For a set \mathcal{S} containing M integer numbers, its cardinality is denoted by $|\mathcal{S}| = M$. In addition, $(\cdot)^*$, $(\cdot)^T$, and $(\cdot)^H$ are the conjugate, transpose, and Hermitian transpose operators, respectively. Finally, \mathbf{I}_N is the $N \times N$ identity matrix, while $\mathbf{X} = \text{diag}\{\mathbf{x}\}$ is a diagonal matrix whose diagonal are the elements of \mathbf{x} .

II. SYSTEM AND CHANNEL MODELS

A. System Model

We consider a time division duplex (TDD) downlink transmission, where a single BS equipped with a DLA of length L communicates with K single-antenna UEs. The direct links between the BS and the UEs are assumed to be blocked, and the communication is facilitated by J RISs, each with M_j UCs forming a uniform linear array (ULA). We denote M as the total number of UCs in all J RISs such that $M = \sum_{j \in \mathcal{J}} M_j$, where $\mathcal{J} = \{1, \dots, J\}$ is a set containing the indices of all RISs. Analytically, the DLA at the BS can also be modeled as a ULA with N critically sampled elements with inter-element spacing of $d = \lambda/2$ [1], where λ is the carrier wavelength. This corresponds to a DLA of length $L = \frac{1}{2}\lambda N$ [2].

We consider a single cell scenario in which the BS is located in the center of the cell which has a radius of R meters, and the J RISs are evenly distributed along the cell circumference. In addition, UEs are randomly located between two circles of radii d_{\min} and d_{\max} meters, as shown in Fig. 1.¹

B. Channel Representation in The Spatial Domain

MmWave MIMO channels can be characterized in a fashion similar to standard multipath channel models. Hence, the spatial domain channel model is expressed in terms of the corresponding array steering vectors that represent the array phase profile. Specifically, considering a ULA with an arbitrary number of antennas or UC elements N_x , one can express the normalized array steering vector for a given angular direction of departing or arriving plane waves as follows [7]:

$$\mathbf{a}(\theta, N_x) = \frac{1}{\sqrt{N_x}} [1, e^{-j2\pi\theta}, e^{-j4\pi\theta}, \dots, e^{-j2(N_x-1)\pi\theta}]^T, \quad (1)$$

where $\theta = \frac{d}{\lambda} \sin(\psi)$ is the spatial frequency, and ψ is the corresponding angle-of-arrival (AoA) or angle-of-departure (AoD). Since the elements are assumed to have half wavelength spacing, the range of values of the spatial frequency is $\theta \in [-0.5, 0.5]$.

The effective cascaded channel in the spatial domain between the BS and all K users, denoted as $\bar{\mathbf{H}} \in \mathbb{C}^{N \times K}$, is:

$$\bar{\mathbf{H}} = \sum_{j \in \mathcal{J}} \mathbf{C}_j \Phi_j \mathbf{G}_j, \quad (2)$$

where $\mathbf{C}_j \in \mathbb{C}^{N \times M_j}$, $\mathbf{G}_j = [\mathbf{g}_{j,1}, \mathbf{g}_{j,2}, \dots, \mathbf{g}_{j,K}] \in \mathbb{C}^{M_j \times K}$, and $\Phi_j = \text{diag}\left\{[e^{j\phi_j}]_1, e^{j\phi_j}]_2, \dots, e^{j\phi_j}]_{M_j}\right\} \in \mathbb{C}^{M_j \times M_j}$ account for the channels between the BS and j th RIS, channels between the j th RIS and all K UEs, and the diagonal phase-shift matrix at the j th RIS, respectively. The k th column of \mathbf{G}_j , denoted as $\mathbf{g}_{j,k} \in \mathbb{C}^{M_j \times 1}$, contains the channel coefficients

¹In our system, UEs are closer to the cell edge than the BS, which justifies the existence of direct links between UEs and RISs. Also, the BS and RISs can be installed on tall buildings with clear line-of-sight (LoS) links.

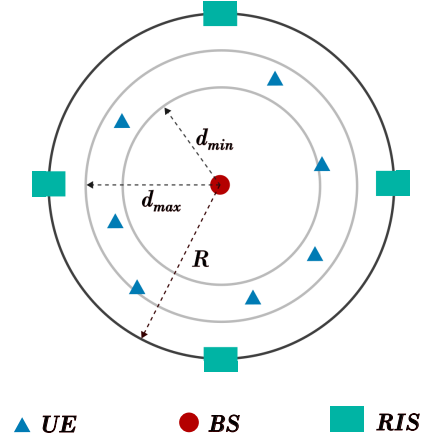


Fig. 1. Illustration of the adopted system model with $J = 4$ and $K = 7$.

between the j th RIS and the k th UE. Assuming an LoS and N_p non-LoS (NLoS) paths for all UEs, $\mathbf{g}_{j,k}$ is expressed as:

$$\begin{aligned} \mathbf{g}_{j,k} &= \mathbf{g}_{j,k,0} + \sum_{l=1}^{N_p} \mathbf{g}_{j,k,l} \\ &= \sqrt{M_j} \eta_{j,k,0} \mathbf{a}(\theta_{j,k,0}, M_j) + \sqrt{\frac{M_j}{N_p}} \sum_{l=1}^{N_p} \eta_{j,k,l} \mathbf{a}(\theta_{j,k,l}, M_j), \end{aligned} \quad (3)$$

where $\mathbf{g}_{j,k,0}$ is the LoS channel vector with $\eta_{j,k,0}$ and $\theta_{j,k,0} = \frac{d}{\lambda} \sin(\psi_{j,k,0})$ being the LoS path gain and direction, respectively. Similarly, $\mathbf{g}_{j,k,l}$ reflects the l th NLoS path, with $\eta_{j,k,l}$ and $\theta_{j,k,l} = \frac{d}{\lambda} \sin(\psi_{j,k,l})$ respectively account for the l th NLoS path gain and direction. Further, the channel between the BS and the j th RIS, denoted as \mathbf{C}_j , is:

$$\begin{aligned} \mathbf{C}_j &= \mathbf{C}_{j,0} + \sum_{l=1}^{N_p} \mathbf{C}_{j,l} \\ &= \sqrt{M_j N} \eta_{j,0} \mathbf{a}(\theta_{j,0}, N) \mathbf{a}(\bar{\theta}_{j,0}, M_j)^H \\ &\quad + \sqrt{\frac{M_j N}{N_p}} \sum_{l=1}^{N_p} \eta_{j,l} \mathbf{a}(\theta_{j,l}, N) \mathbf{a}(\bar{\theta}_{j,l}, M_j)^H, \end{aligned} \quad (4)$$

where $\theta_{j,i} = \frac{d}{\lambda} \sin(\psi_{j,i})$ and $\bar{\theta}_{j,i} = \frac{d}{\lambda} \sin(\bar{\psi}_{j,i})$ correspond to the angles of departure and arrival, respectively, for the i th path with $i \in \{0, \dots, N_p\}$.

C. Channel Representation in The Beamspace Domain

The spatial domain channel matrix $\bar{\mathbf{H}}$ can be transformed into the beamspace domain via the beamforming matrix \mathbf{U} , which reflects the operation of a perfectly designed DLA [2]. Specifically, the N columns in $\mathbf{U} \in \mathbb{C}^{N \times N}$ are steering vectors for N fixed spatial angles having a uniform spacing of $\Delta\theta_0 = \frac{1}{N}$, such that the n th column of \mathbf{U} is expressed as:

$$\mathbf{u}_n = \mathbf{a}(\tilde{n}\Delta\theta_0, N), \quad (5)$$

where $\tilde{n} = (n-1) - 0.5(N-1)$. The matrix \mathbf{U} resembles a Discrete Fourier Transform (DFT) operation, and it is a unitary matrix satisfying $\mathbf{U}\mathbf{U}^H = \mathbf{U}^H\mathbf{U} = \mathbf{I}_N$. The beamspace channel matrix $\mathbf{H} \in \mathbb{C}^{N \times K}$ is obtained as:

$$\mathbf{H} = \mathbf{U}\bar{\mathbf{H}} = \mathbf{U} \sum_{j \in \mathcal{J}} \mathbf{C}_j \Phi_j \mathbf{G}_j. \quad (6)$$

Since \mathbf{U} is unitary, the beamspace channel matrix \mathbf{H} is an equivalent representation of the spatial channel matrix $\bar{\mathbf{H}}$ [1].

Next, we formulate the received signals, signal-to-interference-and-noise ratios (SINRs), the achievable sum rate, as well as the considered optimization problem.

III. RECEIVED SIGNALS, SINRS AND PROBLEM FORMULATION

A. Received Signals

The deployment of a DLA at the BS means that performing signal processing and expressing the received signals can be achieved in the beamspace domain. As such, assuming all N beams are selected, the received signal at the k th UE is:

$$y_k = \sqrt{p_k} \mathbf{h}_k^T \mathbf{w}_k x_k + \sum_{i \in \mathcal{K} \setminus k} \sqrt{p_i} \mathbf{h}_k^T \mathbf{w}_i x_i + n_k, \quad (7)$$

where $\mathcal{K} = \{1, 2, \dots, K\}$ is a set containing the indices of all UEs. Focusing on the k th UE, x_k is the information symbol intended for the UE satisfying $\mathbb{E}\{|x_k|^2\} = 1$, p_k is the amount of power allocated for the UE, $\mathbf{w}_k = \frac{\mathbf{h}_k^*}{\|\mathbf{h}_k\|}$ is the unit-norm MRT precoding vector, and n_k is the additive white Gaussian noise with zero mean and variance of σ^2 . Regarding the second term in the right hand side of (7), it accounts for the inter-user interference.²

B. SINRs and Achievable Rates

The received SINR at the k th UE is given as:

$$\text{SINR}_k = \frac{p_k |\mathbf{h}_k^T \mathbf{w}_k|^2}{\sum_{i \in \mathcal{K} \setminus k} p_i |\mathbf{h}_k^T \mathbf{w}_i|^2 + \sigma^2}, \quad (8)$$

and the achievable rate for the same UE (in bit/s/Hz) is:

$$R_k = \log_2(1 + \text{SINR}_k). \quad (9)$$

Then, the total achievable sum rate can be expressed as follows:

$$\mathcal{R} = \sum_{k \in \mathcal{K}} R_k. \quad (10)$$

C. Problem Formulation

Our aim is to maximize the achievable sum rate via selecting $N_s \geq K$ out of N beams,³ optimizing the phase profile of the J RISs, and optimizing the power distribution for the K UEs. The corresponding optimization problem is given as:

$$\underset{\mathbf{p}, \mathbf{\Phi}, \mathbf{\Delta}}{\text{maximize}} \quad \mathcal{R}(\mathbf{p}, \mathbf{\Phi}, \mathbf{\Delta}) \quad (11)$$

subject to

$$\sum_{k \in \mathcal{K}} p_k \leq P, \quad (12)$$

$$[\mathbf{\Delta}]_{n,n} \in \{0, 1\}, \forall n \in \mathcal{N} \quad (13)$$

$$\sum_{n \in \mathcal{N}} [\mathbf{\Delta}]_{n,n} = N_s, \quad (14)$$

$$|[\mathbf{\Phi}_j]_{m,m}| = 1, \forall j \in \mathcal{J}, \forall m \in \mathcal{M}_j \quad (15)$$

where the objective function $\mathcal{R}(\mathbf{p}, \mathbf{\Phi}, \mathbf{\Delta})$ is given in (16) at the top of the next page, $\mathbf{p} = \{p_1, \dots, p_K\}$, $\mathbf{\Phi} = \{\mathbf{\Phi}_1, \dots, \mathbf{\Phi}_J\}$, $\mathcal{N} = \{1, \dots, N\}$, and $\mathcal{M}_j = \{1, \dots, M_j\}$. Constraint (12) ensures that the total available transmit power at the BS P is not exceeded. The variable $\mathbf{\Delta}$ is a diagonal matrix that controls which beams are

selected. Specifically, in constraint (13), if the n th beam is selected, then $[\mathbf{\Delta}]_{n,n}$ will be equal to 1, otherwise $[\mathbf{\Delta}]_{n,n} = 0$. In addition, constraint (14) ensures that exactly N_s out of the available N beams are selected. Finally, constraint (15) ensures that the unit-modulus constraint at the RIS is not violated. The optimization problem in (11) is highly non-convex due to the unit-modulus constraint, the inter-user interference terms in the objective function, as well as the binary beam selection matrix $\mathbf{\Delta}$, which makes finding the optimal solution an NP-hard problem. To tackle these challenges, we design a low-complexity Metaheuristic approach and perform joint optimization of all optimization variables as described in detail in the next section.

IV. PARTICLE SWARM OPTIMIZATION APPROACH

In this section, we design a low-complexity PSO algorithm to jointly solve the optimization problem in (11). The PSO is a Metaheuristic algorithm that makes few or no assumptions about the problem being optimized. It consists of a population, known as a swarm, of possible solutions (also known as particles). The movement of particles in the search space is influenced by the positions of their local neighbors, as well as the position of the best particle in the swarm, that is, the particle that achieves the best result [8].

In the following subsections, we explain the steps of the proposed PSO algorithm.

A. Initialization

The first step is to randomly initialize the population matrix $\mathbf{F} \in \mathbb{R}^{N_v \times A}$, where $N_v = N + K + M$ is the total number of optimization variables, and A is the number of particles in the population, each representing a possible solution. Considering the a th column in \mathbf{F} , denoted as $\mathbf{f}_a \in \mathbb{R}^{N_v \times 1}$ with $a \in \{1, \dots, A\}$, the first N elements in \mathbf{f}_a , denoted as $[\mathbf{f}_a]_{1:N}$ are associated with the beam selection subproblem. In addition, the elements $[\mathbf{f}_a]_{N+1:N+K}$ are associated with the power allocation subproblem, while the last M elements in \mathbf{f}_a , i.e. $[\mathbf{f}_a]_{N+K+1:}$, are associated with the phase values of all M UCs.

In addition, the velocity matrix $\mathbf{X} \in \mathbb{R}^{N_v \times A}$, which controls the movement and the speed of particles, is initialized with zeros, and will be utilized to update the population as will be seen in subsection IV-E.

B. Constraints Check

Once the population is initialized or updated, its elements must be checked to ensure that no constraints are violated. In the following, we explain how this is done for each subproblem. While our focus in this subsection will be on fixing the entries of a single particle \mathbf{f}_a , the following steps are applied for all A particles in the population.

1) *Beam Selection Constraint:* For each column in \mathbf{F} , the following operation is performed:

$$[\mathbf{f}_a]_n := \frac{|[\mathbf{f}_a]_n|}{\max\{|[\mathbf{f}_a]_1|, \dots, |[\mathbf{f}_a]_N|\}}, \quad \forall n \in \{1, \dots, N\}. \quad (17)$$

The normalization in (17) ensures that for each particle, all N entries corresponding to the beam selection subproblem are positive and within the range $[0, 1]$.

2) *Power Allocation Constraint:* The entries corresponding to the power allocation subproblem are normalized as follows:

$$[\mathbf{f}_a]_n := \frac{|[\mathbf{f}_a]_n|}{\sum_{i=N+1}^{N+K} |[\mathbf{f}_a]_i|} \times P, \quad \forall n \in \{N+1, \dots, N+K\}. \quad (18)$$

In (18), we ensure that the amount of power allocated for each UE is positive, and the total transmit power for all UEs is equal to P .

3) *RIS Profile Constraint:* The final step is to adjust the phase-shift values of all M UCs to be within the range $[0, 2\pi]$ as follows:

$$[\mathbf{f}_a]_n := \begin{cases} [\mathbf{f}_a]_n + 2\pi, & \text{if } [\mathbf{f}_a]_n < 0 \\ [\mathbf{f}_a]_n - 2\pi, & \text{if } [\mathbf{f}_a]_n > 2\pi, \end{cases} \quad (19)$$

$\forall n \in \{N+K+1, \dots, N_v\}$.

²We assume a perfect knowledge of channel state information (CSI).

³The number of required RF chains at the BS is equivalent to the number of selected beams. Since there are K UEs, N_s cannot be smaller than K .

$$\mathcal{R}(\mathbf{p}, \Phi, \Delta) = \sum_{k \in \mathcal{K}} \log_2 \left(1 + \frac{p_k \left| \left(\mathbf{U} \sum_{j \in \mathcal{J}} \mathbf{C}_j \Phi_j \mathbf{g}_{j,k} \right)^T \Delta \frac{(\mathbf{U} \sum_{j \in \mathcal{J}} \mathbf{C}_j \Phi_j \mathbf{g}_{j,k})^*}{\|\Delta \mathbf{U} \sum_{j \in \mathcal{J}} \mathbf{C}_j \Phi_j \mathbf{g}_{j,k}\|} \right|^2}{\sum_{i \in \mathcal{K} \setminus k} p_i \left| \left(\mathbf{U} \sum_{j \in \mathcal{J}} \mathbf{C}_j \Phi_j \mathbf{g}_{j,i} \right)^T \Delta \frac{(\mathbf{U} \sum_{j \in \mathcal{J}} \mathbf{C}_j \Phi_j \mathbf{g}_{j,i})^*}{\|\Delta \mathbf{U} \sum_{j \in \mathcal{J}} \mathbf{C}_j \Phi_j \mathbf{g}_{j,i}\|} \right|^2 + \sigma^2} \right). \quad (16)$$

C. Evaluate the Quality of Particles

After we ensure that all constraints are met, we evaluate the quality, which in this case is the achievable sum rate in (16), of each particle. Focusing on an arbitrary particle \mathbf{f}_a , the evaluation involves performing the following steps:

1) *Construct the RISs Profile Matrices:* The first step is to construct the response of the J RISs with the optimized phase shifts. We denote $\Phi(a) = \{\Phi_1(a), \dots, \Phi_J(a)\}$ as the RISs profile matrices where the response of all RISs are obtained from \mathbf{f}_a as:

$$\Phi_j(a) = \left\{ \Phi_j \left[[\phi_j]_1, \dots, [\phi_j]_{M_j} \right] = [\mathbf{f}_a]_{z_j+1:z_j+M_j} \right\}, \quad (20)$$

where $z_j = N + K + \sum_{i=1}^{j-1} M_i$, and $j \in \mathcal{J}$.

2) *Selection of N_s Beams:* For each particle, we select the N_s beams with the highest values in $[\mathbf{f}_a]_{1:N}$ as follows:

$$\mathcal{S}(a) = \arg \max_{N_s} \{[\mathbf{f}_a]_1, \dots, [\mathbf{f}_a]_N\}, \quad (21)$$

where $\mathcal{S}(a)$ is the set of indices of selected beams for particle \mathbf{f}_a , with cardinality $|\mathcal{S}(a)| = N_s$. Then, the diagonal elements in $\Delta(a)$ that correspond to the N_s values in $\mathcal{S}(a)$ are set to 1, while the remaining $N - N_s$ diagonal elements in $\Delta(a)$ are set to 0. It should be noted that $\Delta(a)$ denotes the diagonal binary beam selection matrix Δ for the a th particle. Analytically, the relation between $\Delta(a)$ and $\mathcal{S}(a)$ can be expressed as:

$$[\Delta(a)]_{n,n} = \begin{cases} 1, & \text{if } n \in \mathcal{S}(a) \\ 0, & \text{otherwise,} \end{cases}, \forall n \in \mathcal{N}. \quad (22)$$

3) *Power Allocation:* The final step before evaluating the quality is to obtain the power allocated for each UE as follows:

$$p_k(a) = [\mathbf{f}_a]_{N+K}, \quad \forall k \in \{1, \dots, K\}. \quad (23)$$

For the a th particle, we denote the set of power values for all UEs as $\mathbf{p}(a) = \{p_1(a), \dots, p_K(a)\}$.

4) *Sum Rate Evaluation:* Now we can evaluate the quality (i.e. the achievable sum rate) of the a th particle by substituting $\mathbf{p} = \mathbf{p}(a)$, $\Phi = \Phi(a)$, and $\Delta = \Delta(a)$ in (16).

D. Find Local and Global Best Solutions

Once the qualities of all A particles are evaluated, we find the local and global best solutions. Specifically, the global best solution is the particle in \mathbf{F} that achieves the highest sum rate. We denote the global best solution as \mathbf{f}_{gb} .

On the other hand, the local best solution for the a th particle is the particle that achieves the highest sum rate between only the two neighboring particles of \mathbf{f}_a , which are \mathbf{f}_{a+1} and \mathbf{f}_{a-1} .⁴ We denote the local best solution for the a th particle as $\mathbf{f}_{lb,a}$.

⁴We adopt a ring topology for the particles. Hence, the neighboring particles of \mathbf{f}_1 are \mathbf{f}_2 and \mathbf{f}_A , while the neighbors of \mathbf{f}_A are \mathbf{f}_1 and \mathbf{f}_{A-1} .

E. Update the Population

The final step is to update the population. This is performed over two stages. At first, the velocity of the population \mathbf{X} is updated as:

$$\begin{aligned} [\mathbf{X}]_{i,a} := & \mu [\mathbf{X}]_{i,a} + w_1 * rand_1 ([\mathbf{f}_{gb}]_i - [\mathbf{f}_a]_i) \\ & + w_2 * rand_2 ([\mathbf{f}_{lb,a}]_i - [\mathbf{f}_a]_i), \end{aligned} \quad (24)$$

where $a \in \{1, \dots, A\}$, $i \in \{1, \dots, N_v\}$, $rand_1$ and $rand_2$ are random numbers between 0 and 1 drawn from a uniform distribution, w_1 and w_2 are learning factors, and μ is the inertia weight.

Next, the population matrix is updated as:

$$\mathbf{F} := \mathbf{F} + \mathbf{X}. \quad (25)$$

F. Iterate

The operations explained in IV-B to IV-E are for a single iteration of the PSO algorithm. Therefore, the same steps IV-B to IV-E will be repeated T times, where T is the total number of optimization iterations. At the end, the particle that achieves the highest sum rate across all T iterations will be selected as the final solution.

It is worth mentioning that the proposed PSO approach has a per-iteration complexity order of $\mathcal{O}(A \cdot N \cdot M \cdot K)$.

V. SIMULATION RESULTS

A. Channel Parameters and Path-Loss Model

We adopt the Urban Micro (UMi) path-loss (PL) model in [9, Table 7.4.1-1]. For any two arbitrary nodes i and j , the corresponding PL, denoted as $\zeta_{i,j}$, can be expressed as

$$\zeta_{i,j} [\text{dB}] = \begin{cases} 32.4 + 21 \log_{10}(d_{i,j}) + 20 \log_{10}(f_c), & \text{if LoS} \\ 32.4 + 31.9 \log_{10}(d_{i,j}) + 20 \log_{10}(f_c), & \text{if NLoS} \end{cases} \quad (26)$$

where f_c is the operating frequency in GHz, and $d_{i,j}$ reflects the distance in meters. The values of η in (3) and (4) are then obtained as $\eta_{i,j,0} = \sqrt{10^{-\frac{\zeta_{i,j}}{10}}}$ for the LoS, and $\eta_{i,j,l} = \sqrt{10^{-\frac{\zeta_{i,j}}{10}}} e^{-j2\pi\vartheta_l}$ for the NLoS, where ϑ_l is uniformly distributed between 0 and 2π . In addition, the AoAs at RISs are drawn from a uniform distribution between $-\pi/2$ and $\pi/2$, while the AoDs from the BS as well as the AoAs at all UEs are uniformly distributed between $-\pi$ and π .

B. Simulation Parameters

Unless stated otherwise, the following set of parameters where adopted in the simulations: The carrier frequency $f_c = 30$ GHz, the noise variance $\sigma^2 = -110$ dBm, number of RISs $J = 8$, number of UEs $K = 8$, cell radius $R = 40$ meters with $d_{min} = 25$ meters and $d_{max} = 35$ meters, number of NLoS paths $N_p = 2$, number of DLA elements $N = 64$, total transmit power $P = 40$ dBm, the number of selected beams $N_s = 8$, and $M_j = M/J \forall j \in \mathcal{J}$. In addition, for the PSO algorithm, the number of particles $A = 50$, the number of iterations $T = 200$, the inertia weight $\mu = 0.05$, and the PSO learning parameters $w_1 = w_2 = 2$. Simulations are averaged over 1000 independent channel realizations and UEs locations.

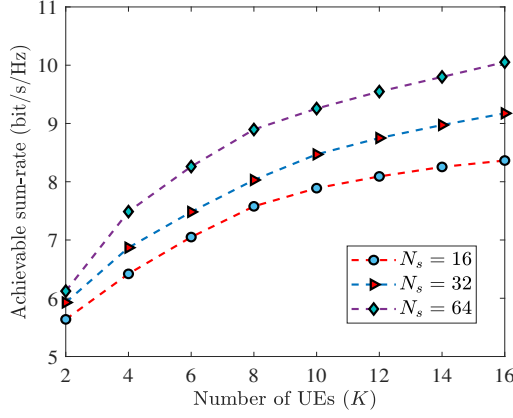


Fig. 2. Achievable sum-rate vs. number of UEs for different number of selected beams when $M = 128$.

C. Discussions

Fig. 2 shows the sum rate for different numbers of UEs and selected beams. Accommodating a larger number of UEs leads to higher achievable sum rates. In addition, the results reflect the key advantage of the beamspace MIMO which relies on high channel sparsity. In particular, as the number of selected beams increases, a relatively small increase in the total sum rate is observed. For example, when $K = 16$, the sum rate increases by only 0.8 bits/s/Hz when the number of N_s is doubled from 16 to 32.

The efficiency of the proposed PSO algorithm can be seen in Fig. 3, which shows the achievable sum rate as a function of the number of PSO iterations. It should be noted that when the number of iterations is equal to zero, the results reflect the achievable sum rate with random solutions of selected beams, allocated powers, and phase-shifts of UCs. For the case where $M = 256$, the proposed PSO scheme provides more than 7 bit/s/Hz improvement compared to the random solution after 200 optimization iterations, and more than 8 bit/s/Hz after 400 iterations. Furthermore, it can also be observed that increasing the number of optimization variables (in this case M) affects the convergence behavior of the PSO algorithm. Specifically, the PSO algorithm requires a larger number of iterations to converge when the number of optimization variables increases. This behavior is natural due to the larger search space the PSO needs to explore when increasing the number of optimization variables.

Finally, we observe from Fig. 2 and Fig. 3 that increasing the number of UCs is preferred to increasing the number of selected beams. For example, increasing N_s from 32 to 64 corresponds to an increase of 0.9 bit/s/Hz in the sum rate (or even less, depending on the number of UEs). In contrast, increasing M from 32 to 64 can lead to a sum rate that is 2 bit/s/Hz higher. This is due to the sparsity of the beamspace channels. More specifically, increasing the number of beams will result in additional channel vectors that are likely not well aligned with the directions of RISs, and thus have low channel gain. In contrast, increasing the number of UCs M can enhance the channel gain for beams pointing toward the directions of RISs. This brings significant advantages in terms of energy efficiency, as increasing the number of beams means more power-hungry RF chains at the BS, while incorporating additional UCs at RISs does not require additional RF chains.

VI. CONCLUDING REMARKS

The performance of a multi-RIS-aided mmWave beamspace MIMO with multiple UEs was investigated in this work. A low-complexity algorithm based on the PSO approach was designed to jointly optimize the selection of beams, allocation of powers, and

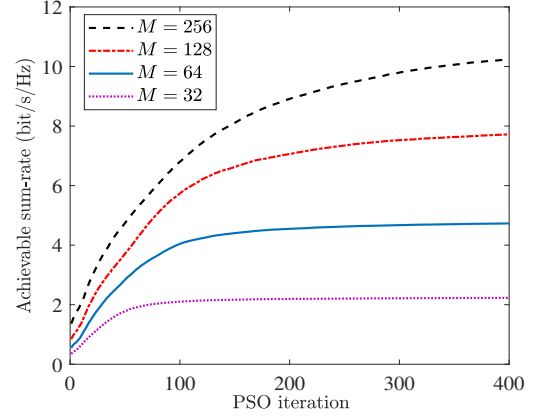


Fig. 3. Convergence of the proposed PSO scheme, $K = N_s = 8$.

configuration of the multiple RISs. Numerical results demonstrated the efficiency of the proposed optimization approach, and highlighted key complexity-performance trade-offs. It was also demonstrated that with beamspace MIMO, one should aim for larger RISs rather than activating more beams at the MIMO BS, which could result in significant gains in terms of the energy efficiency performance.

ACKNOWLEDGMENT

This work has been supported by the Smart Networks and Services Joint Undertaking (SNS JU) project TERRAMETA under the European Union's Horizon Europe research and innovation programme under Grant Agreement No 101097101, including top-up funding by UK Research and Innovation (UKRI) under the UK government's Horizon Europe funding guarantee.

REFERENCES

- [1] A. Sayeed and J. Brady, "Beamspace MIMO for high-dimensional multiuser communication at millimeter-wave frequencies," in *IEEE global Commun. Conf. (GLOBECOM)*, 2013, pp. 3679–3684.
- [2] P. V. Amadori and C. Masouros, "Low RF-complexity millimeter-wave beamspace-MIMO systems by beam selection," *IEEE Trans. Commun.*, vol. 63, no. 6, pp. 2212–2223, 2015.
- [3] E. Basar *et al.*, "Wireless communications through reconfigurable intelligent surfaces," *IEEE Access*, vol. 7, pp. 116 753–116 773, 2019.
- [4] Y. Wang *et al.*, "Intelligent reflecting surface-assisted mmWave communication with lens antenna array," *IEEE Trans. Cog. Commun. Net.*, vol. 8, no. 1, pp. 202–215, 2021.
- [5] T. Y. Elgarni *et al.*, "IRS-assisted beamspace millimeter-wave massive MIMO with interference-aware beam selection," in *IEEE 96th Veh. Technol. Conf. (VTC2022-Fall)*, 2022, pp. 1–6.
- [6] D. Alimo and M. Hamamura, "Low-complexity beam selection for intelligent reflecting surface-aided millimeter-wave systems with lens antenna array," in *IEEE 98th Veh. Technol. Conf. (VTC2023-Fall)*, 2023, pp. 1–5.
- [7] R. W. Heath *et al.*, "An overview of signal processing techniques for millimeter wave MIMO systems," *IEEE J. Sel. Topics Sig. Process.*, vol. 10, no. 3, pp. 436–453, 2016.
- [8] J. Kennedy and R. Eberhart, "Particle swarm optimization," in *Proc. IEEE Int. Conf. Neural Nets.*, vol. 4, 1995, pp. 1942–1948.
- [9] Third generation partnership project (3GPP), "3GPP TR 38.901: Study on channel model for frequencies from 0.5 to 100 GHz," Release 17, V17.1.0, Tech. Rep., Dec. 2023. [Online]. Available: <https://www.3gpp.org/dynareport/38901.htm>